Chapter 19
The Grain-Size Distribution of Rock-Avalanche Deposits: Implications for Natural Dam Stability

Stuart A. Dunning and P.J. Armitage

1 Introduction

Rock avalanches are a catastrophic mass movement derived from the failure of a commonly agreed upon minimum volume of 1×10^6 m^3 of bedrock and associated cover material. The initial failure may initiate as a rockslide, topple or poly-phase event, but transitions to a rock avalanche leaving behind a characteristic granular deposit. The mechanisms of motion that allow rock avalanches to achieve runout distances that are considered excessive are at present unknown, but has been, and still is, the focus of intense research providing a multitude of possible solutions. Historically, in this search for a global mechanism for the runout of rock avalanches the sedimentology of rock-avalanche deposits has often been overlooked at best, poorly described at worst yet the field features are now beginning to drive theories of how they move [7].

As "natural", non blast triggered (cf. Chap. 25 by Adushkin, and Chap. 26 by Korchevskiy et al., this volume) rock avalanches cannot be predicted, monitored or instrumented and are rarely witnessed, it is the resulting rock-avalanche deposit that can provide the best insight into the final moments of motion and the possible processes acting during "flow".

Rock avalanches primarily occur in the high mountains of the world [17], and, after failure travel to valley floors, often impacting upon the drainage network over human [8, 9] and geological timescales [14]. Rock-avalanche deposits are capable of creating high and wide, valley-blocking dams by virtue of their volume and capability to run-out for considerable distances across and down valley. Of the reported landslides that create dams, rock-avalanche deposits are one of the most common forms [3]. Of concern is that is that *if* a landslide dam does fail, it usually does so rapidly; it has been calculated that of those that fail, 50% will fail within 10 days of formation [3]. For those that last above these short-term thresholds, the time to

S.A. Dunning (✉)
Discipline of Geography and Environment, Northumbria University, Newcastle Upon Tyne NE1 8ST, UK
e-mail: stuart.dunning@northumbria.ac.uk

S.G. Evans et al. (eds.), *Natural and Artificial Rockslide Dams*, Lecture Notes in Earth Sciences 133, DOI 10.1007/978-3-642-04764-0_19, © Springer-Verlag Berlin Heidelberg 2011

Fig. 19.1 Preserved banding sub-facies at the Falling Mountain rock-avalanche deposit consisting of highly fragmented, angular, fine, bands of dark argillite and highly fragmented, angular, coarse, light coloured greywacke. Highly fractured but relatively undisaggregated clasts are common; a large greywacke example is highlighted. The boundaries between bands are sharp with no evidence of mixing. Height of river-cut exposure is approximately 4 m

failure may be measured in years, decades, or even centuries [13] and may never "fail" but slowly erode. Of the factors relating to the stability of a rock-avalanche dam the material properties are deemed critical [3], sensibly based on the history of engineering experience of earth-fill dams.

It appears that as with the mechanisms of motion for rock avalanches, landslide-dam stability study has much to gain from studies of the sedimentology of the resulting deposits. The current state of knowledge adheres to commonly described features; crude inverse grading [5, 13], highly fractured but relatively undisaggregated clasts (Figs. 19.1 and 19.2) [6], preservation of source stratigraphy in the final deposit (Fig. 19.1), and, interaction with the deposit substrate [16].

2 Methodology

Recent sedimentological studies have attempted to plug the gaps in current knowledge with a variety of techniques, based on either direct sampling [2, 4] or an observational, facies based approach [20]. Numerous problems persist in the attempt to characterise rock-avalanche sedimentology, not least of which is the issue of how truly representative any sampling regime can be. The presumed minimum volume above which characteristic rock-avalanche sedimentology can be observed is 1×10^6 m^3; to sample just 1% of this minimum mass would involve sieving of 10,000 kg of debris, at the Flims rock-avalanche deposit, more than 1,000,000 kg of debris for a point sample. Any direct sampling regime has to accept this inherent

Fig. 19.2 Close up view of a highly fractured but undisaggregated greywacke clast at the Falling Mountain rock-avalanche deposit. Distinct "impact" marks are preserved with fractures radiating away from them. These features must have either been transported without the fractures opening and allowing matrix infill and further fracture as observed in Fig. 19.1; or, this represents a fracture event immediately before the cessation of motion of the rock avalanche

problem and be appropriate to the features observed. Rock-avalanche deposits are not simple, structureless, breccias; they preserve original source stratigraphy in the final deposit, often many kilometres from that source. Another common observation is that of crude inverse grading of deposits from a finely fragmented interior to a blocky openwork surface. For these reasons, a random sampling regime should not be applied to any direct sampling of rock-avalanche deposits. Significant variations in sedimentology must be related directly to the features observed or measured, this requires biased sampling, be that towards preserved lithological band types and their boundary effects, grading, height in deposit or distance along flow.

For this research, data from five rock-avalanche deposits have been identified for biased direct sampling; Acheron [21], Falling Mountain [18], Poerua [11, 12], and Round Top [25] in New Zealand, and the Flims rock-avalanche deposit [20] in the Swiss Alps. The volumes involved vary by orders of magnitude but all can be described as valley-confined (TYPE II, III of Costa and Schuster [3],) or down-valley directed. Sampling used a combination of field and laboratory sieving along with laser granulometry for a least errors method [24]. Individual sample sizes were in the order of 15–20 kg and deemed sufficient to determine the grain-size distribution (GSD) of the site-specific features studied and to yield comparative data between and within deposits. A maximum clast size of 256 mm and minimum of 0.002 mm is characterised using this technique; no clasts in the *interior* of deposits sampled exceeded this maximum size. The raw GSD data obtained has been entered into a sedimentological analytical package to calculate the standard suite of descriptive statistics [1].

Further analysis utilised model fitting methods, using the techniques of [15] to test for a fractal distribution of the data and of [23] for a Weibull (Rosin-Rammler) type distribution as described previously for rock avalanche GSDs [22].

3 The Grain Size Distribution of Rock-Avalanche Deposits

It rapidly becomes apparent from field observations and data analyses that the preserved stratigraphy found in the interior of deposits is a key control on the GSD. Individual lithologies have GSDs that are significantly different from one another yet remarkably consistent between layers of the same rock type at a site. This can be illustrated with GSD data derived from the Flims rock-avalanche deposit (Fig. 19.3) composed of distinct, alternating preserved bands of dark and light coloured calcareous Jurassic Malm limestone. The GSDs segregates on preserved lithological band type over any other tested variable, this includes height in deposit and distance along flow path (although this is complicated by topographic confinement). It is the lithological and stratigraphic composition of the source region for a deposit that dominates the final GSD and overprints any down-flow fining trends. This lithological control is found to be true for all sampled deposits where the source stratigraphy allows for recognition in the final deposit of distinct preserved rock types.

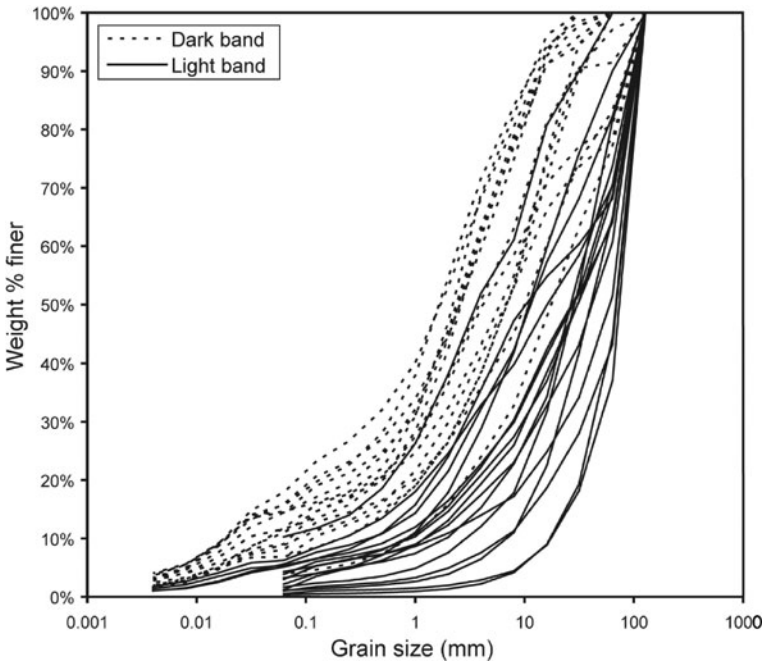

Fig. 19.3 Grain size distributions for samples taken from the Flims rock-avalanche deposit by preserved band type

Table 19.1 The range of values for selected descriptive statistics based on five rock-avalanche deposits of varied lithology

	N	Minimum	Maximum	Mean	SD
Mean (Phi)	89	−0.13	−5.69	−2.63	1.31
Median (Phi)	89	−0.82	−6.19	−3.24	1.36
Sorting (Phi)	89	1.46	3.69	2.60	0.48
Gravel (%)	89	46.97	98.65	75.85	0.10
Fractal dimension	89	1.95	3.04	2.44	0.20

All of the deposits sampled display finely skewed GSDs and can be classed as poorly to very-poorly sorted. A range of descriptive statistics derived from the GSD can be summarized as data ranges (Table 19.1) and as a gravel-sand-clay plot showing the possible and most likely GSD assemblages (Fig. 19.4). Each sample GSD has been tested using both a Weibull approach and a fractal approach. All samples tested prove to be fractally distributed, the range of values are shown in Table 19.1. The fractal dimension of samples increases with decreasing grain size and achieves a maximum value of 3.04 approaching values of both natural and simulated fault gouges [19]. Application of a Weibull distribution [23] has not proven successful and only fits over an extremely limited portion of the GSD of a sample. Examples of both methodologies applied to a single sample are shown in Figs. 19.5 and 19.6.

The notion of inverse grading of rock-avalanche deposits can be tested at several of the sampled sites. Data from the Falling Mountain rock-avalanche deposit (Fig. 19.7) is presented as an example of the findings. The Falling Mountain exposure presented is located 3 km from the source region and is a near full basal to

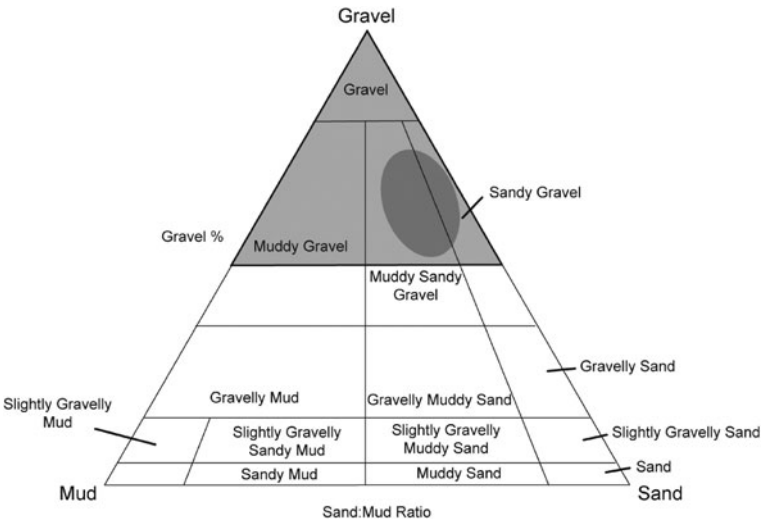

Fig. 19.4 Gravel-sand-mud plot for the possible (*light*) and usual (*dark*) grain size assemblages for rock-avalanche deposits based on 89 samples from 5 rock-avalanche deposits

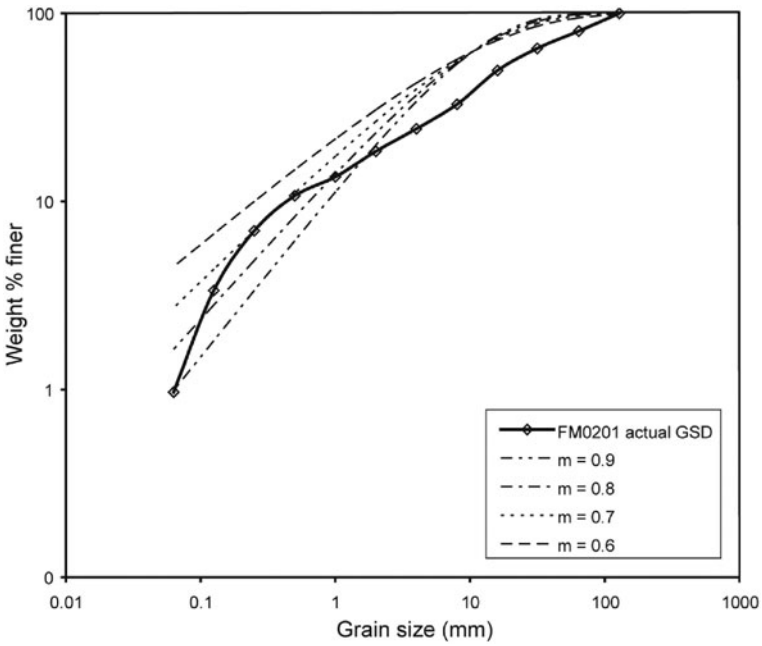

Fig. 19.5 Application of the Weibull distribution [15] to a sample from the Falling Mountain deposit varying the exponent *m*

surface exposure composed of fine dark argillite bands and coarser, light coloured greywacke, preserved sub-horizontal bands, similar to those observed in the source region, although in the source the bedding is near to vertical suggesting stretching and rotation. It is apparent from Fig. 19.7 that the interior of the Falling Mountain rock-avalanche deposit is not inversely graded, and this is true of all sites studied with such exposures where the deposits have spread and fragmented extensively. The variations in GSD and median, mean or modal grain size are directly related to the preserved lithological band type a sample is removed from. Comparisons of similar lithological band types at varied heights in the section also show no indication of coarsening upwards. The only instances of grading are within thicker units, for example the near-basal greywacke unit (Fig. 19.7); this grading is normal in nature, that is to say becoming finer grained upwards, and it cannot be ascertained if this is an emplacement feature or representative of source rock features. The same trend has been observed at the Flims rock-avalanche deposit within the thicker preserved units. The abnormally coarse unit at the top of the Falling Mountain exposure (Fig. 19.7) is argillite that composes the deposit surface and near surface at this point as a carapace. This unit is sharply bounded below against another, far finer argillite unit. There is no grading between the two units; the surface layer is separate and distinct in its GSD.

Variations in grain size, unrelated to source rock strength/lithology are also observed for the distance from source at Falling Mountain. Proximal exposures

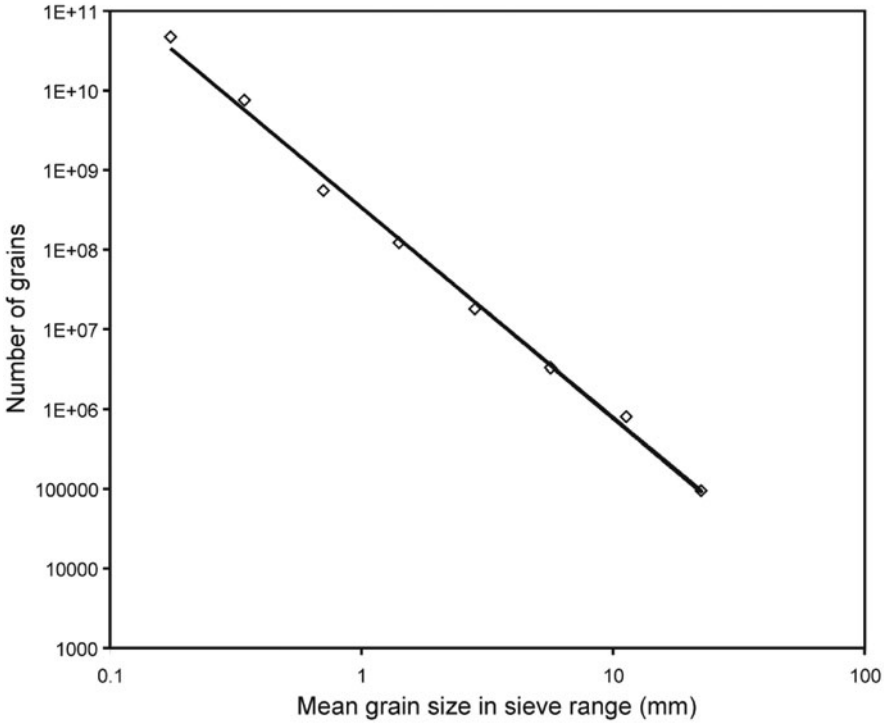

Fig. 19.6 Application of the fractal method to the same sample as Fig. 19.5. The resulting fractal dimension yielded by the line of best fit is 2.64 with an r^2 value of 0.99

show coarse GSDs dominated by very coarse gravel and larger, more distal exposures show a fining of this GSD for the same rock types with a decreasing gravel content (absolute loss of coarse grades). This is a complex phenomena, the results are clearest in the simple case of a rock avalanche leaving the source region and travelling, confined, along a valley such as at Falling Mountain. Deposits of considerable size, or those that spread across and along wide valleys in multiple directions, show far more complicated relationships such as at Flims.

4 A Simplified Facies Model for Rock-Avalanche Deposits

Detailed field investigations in combination with GSDs from the interior of the deposits presented above reveal that the deposits investigated are not inversely graded but at their simplest show three distinct facies; a surface and near surface carapace facies, the main interior body facies, and a basal facies that includes the regions of the interior that have incorporated substrate material or are affected by it. A detailed description of the facies is beyond the scope of this paper and for the purposes of this study only a brief summary is required.

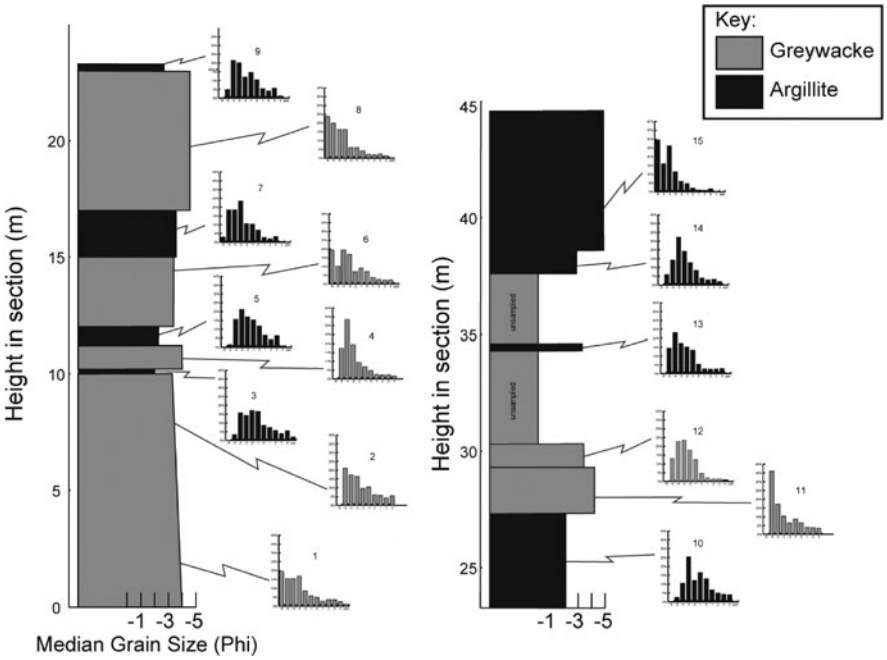

Fig. 19.7 Graphical log through a section of the Falling Mountain rock-avalanche deposit. The exposure is composed of coarser greywacke units and finer argillite units banded sub-horizontally

4.1 The Carapace Facies

The carapace facies is the coarsest unit of a rock-avalanche deposit and is the material composing the surface and near surface, observations suggest a depth of up to 30% of total-deposit thickness as a maximum in deposits that have not been prematurely stalled by topography. The facies is clast supported and retains source stratigraphy as discreet bands without mixing. This is often obscured as the surfaces of rock-avalanche deposits, particularly proximal regions, can exhibit lobes of material orientated toward the source, interpreted to represent "pulses" of debris in the final stages of failure. The key point of relevance is that the facies is sharply bounded below (Fig. 19.7), with the boundary defined as the line below which all material is intensely fragmented, matrix supported and showing fragmentation derived features – the body facies. Observational and experimental evidence suggest that the carapace facies may show inverse grading but this is a near surface phenomena and not representative of the entire depth of deposit. Deposits that are relatively thin, either through runout of a low volume of material (Acheron for example), or through unconfined spreading, may consist almost entirely of the carapace facies. For reasons like this it is, entirely understandable that observations/measurements have been made on the "inverse grading" of deposits, since it is often either an exposure primarily of a graded carapace or an

erroneous observation made on the basis of a coarse near surface, a fine interior and qualitative assumptions of grading between the two. The carapace facies is of critical importance to rock-avalanche dam stability because it is the material forming the dam crest, and is of course the only material available for observation on arrival at a recent event requiring urgent hazard assessment.

4.2 The Body Facies

The body facies forms the main body of rock-avalanche deposits and is usually the most voluminous in valley-confined deposits that have undergone significant runout. Features of note include, highly fractured but relatively undisaggregated clasts, matrix support, impact marks with radial fracture preserved on clasts (Fig. 19.2), and as described, preserved source stratigraphy, although orientations and thicknesses are considerably altered. A number of sub-facies can be identified within the body facies but they are outside of the scope of this paper and more related to variations in fragmentation and topographic confinement.

4.3 The Basal Facies

This base of a rock-avalanche deposit is rarely exposed, and never in the case of hazard assessment planning at recent dam forming deposits. The basal facies not only includes rock-avalanche material that is interpreted to have interacted with the substrate, but also the substrate material altered by passing rock avalanche, including that bulldozed in front of the rock avalanche. This includes erosion and entrainment of substrate material into the base of the moving debris, and also subsequent deposition of modified mixes of substrate and rock-avalanche material. This is of course substrate dependant, be it soft erodable valley fills and surface vegetation that can be carried for some distance, or regions of bedrock that undergo superficial erosion as the mass passes – a good example being the bedrock gorge at Falling Mountain, subsequently re-exhumed by erosion of the rock-avalanche deposit. The boundary between the basal facies and the body facies is often indistinct and variable in its height above the assumed deposit base. The facies is, however, interpreted to be the smallest by volume within a rock-avalanche deposit, although in deposits that have spread and thinned completely unrestricted over deformable substrates it may only be the basal and carapace facies that remain.

5 Discussion

The results of a sedimentological study provide a number of new advances in the field as well as interpretations that take the study beyond the simply descriptive. Detailed description has been required for the sedimentology of rock-avalanche

deposits, be they dam forming or not. Many past, and current models of their mechanisms of motions ignore these first principles of field study; models should fit with quantified deposit features rather than simply being a "black box" approach that may yield the required travel distance or dam-overtopping time, without consideration of the deposit features and sedimentology. It can be hoped that usage of a facies approach and the GSD data presented allows a brief glimpse into the sedimentology of rock-avalanche deposits. The data raise questions on how to relate initial source rock strength to final deposit GSD, and the effect of multiple lithological units. Deposits such as Falling Mountain show clear fragmentation segregation, fragmentation is far more intense along the weaker argillite layers that have correspondingly higher fractal dimensions resembling fault gouge. Investigation will reveal if this is simply a response to the relative strengths and initial fracture distribution of the source rock, or if in fact the fragmentation does localise in the weaker units. All interior rock-avalanche GSDs prove fractal in this study and those selected and tested from the literature where sampling methodology allows. This in essence shows that rock-avalanche deposit interiors are self-similar at scales of observation. The values of the fractal dimension of the rock-avalanche GSDs vary (Table 19.1) but all show an average of ~2.44. This is below the value of 2.58 interpreted to represent equal probability of fracture across all size grades, a configuration representing maximal spacing of same size clasts [19]. Values above 2.58 are interpreted to represent configurations with an excess of fines [19]. It can be interpreted for the rock-avalanche deposits studied that there is an excess of coarse material, that motion has stopped before maximal "cushioning" of same-size clasts could be achieved. It also follows that the deposits studied were, immediately prior to the cessation of motion, preferentially fragmenting these coarser clasts. This is backed by the fining of rock-avalanche deposits with distance from the source (an absolute loss of coarse grades) and a significant statistical relationship showing that as grain size becomes finer, the fractal dimension increases, becoming closer to the 2.58 value. Observations show that maximal "cushioning" has not been achieved, i.e., there are numerous fragmented but relatively undisaggregated clasts at all distances from the source. These can be interpreted to either represent transported fragmentation events that occurred near the source; or, they represent fragmentation events immediately prior to stopping. Those with significant matrix infill in the fractures represent may slightly older fragmentation events.

6 Application of the Data to Rock-Avalanche Dams

6.1 Prediction of Parameters

The data set presented is important for the study of rock-avalanche dams in a number of ways. Firstly, and possibly most importantly, it provides the GSD and basic properties of the material forming the dam, something that has previously been reported as critical [3]. The distinction of a carapace facies and body facies allows for an

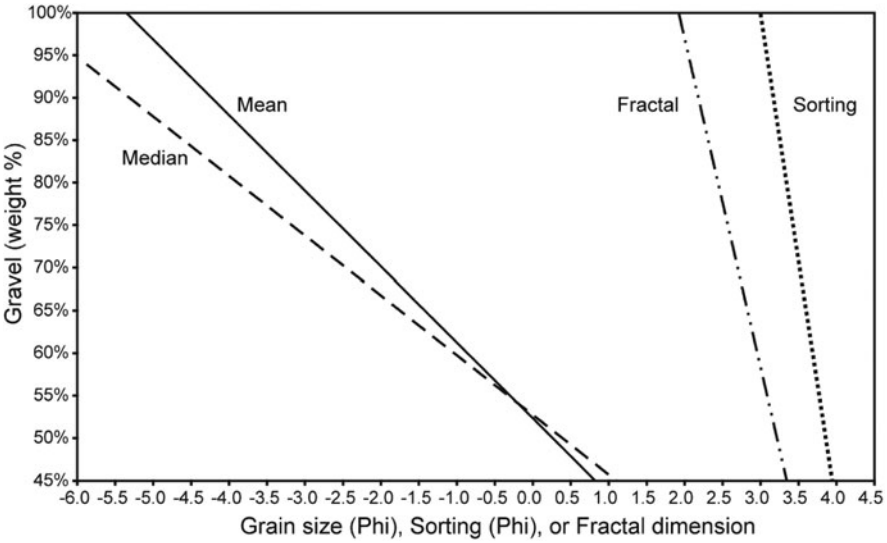

Fig. 19.8 Predictive plot generated after study of rock-avalanche deposit interiors to calculate mean and median grain sizes (Phi), fractal dimension, or sorting (Phi) based on statistical relation to weight percent gravel. The plot can be used to calculate each parameter from any single measurement; mean, median or weight percent gravel are the recommended inputs

estimation of the properties of the material unobserved on arrival at a recent rock-avalanche dam forming deposit. Preliminary results for similar data in the carapace facies, taken in a relatively fine grained carapace formed from argillite at Falling Mountain, allow for conservative values to compare against the main interior values. For estimation of the properties of any particular rock-avalanche dam, predictive plots have been generated (Figs. 19.8 and 19.9) based on a simple measure or estimation of weight percent gravel. From these, values of mean and median grain size, sorting, fractal dimension, and permeability can be estimated. Deposits vary in their relative coarseness by lithology. Although the relationships to weight percent gravel are applicable for all lithologies, more discreet zones of lithology are required so that even the simple measure/estimation of gravel is no longer required for rapid assessment.

6.2 Data Used for Modelling

Grain size data is a key component in various dam break/dam breach software packages. These models use inputs such as median grain size of the material composing the dam interior and exterior to calculate the rate of dam crest breaching via overtopping – the most common cause of landslide dam failure [3]. However, the sedimentology presented above, with its distinct differences between the dam crest formed of the carapace facies and the main bulk formed of the body facies

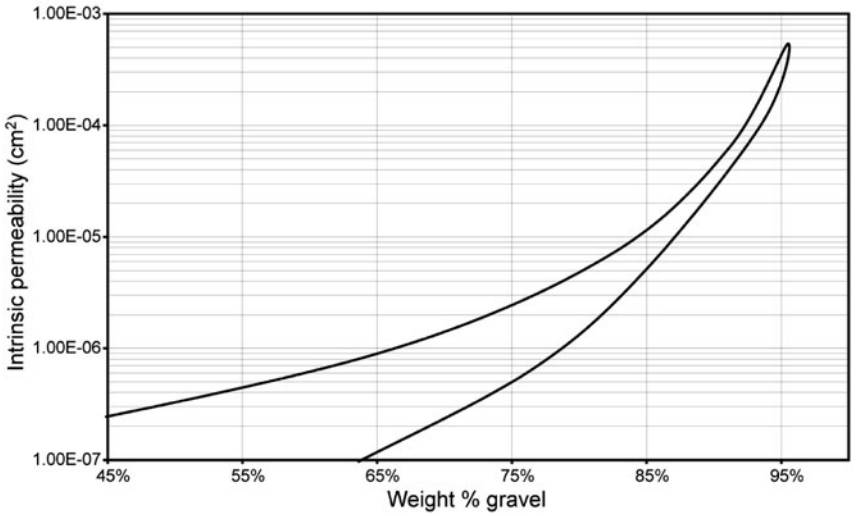

Fig. 19.9 Predictive plot showing the range of intrinsic permeability for rock-avalanche deposits based upon a measure of weight percent gravel. Alternative plot for hydraulic conductivity is also available based on the data set

raise some interesting questions. From the GSD it is possible to calculate simple approximations of the hydraulic conductivity and intrinsic permeability (Fig. 19.9) and, from density measurements and wetting/drying experiments, it is possible to calculate porosity of the debris assemblage. These properties, along with several that are more calculable from case-study examples, allow us to begin to assess the role of sedimentology on dam stability. Although rock-avalanche dams are commonly assumed to fail during overtopping, it is interesting to study the process of the impounded lake filling against the dam until that overtopping since the final failure mechanism may actually be face-failure rather than overtopping (which should be confined to the headward erosive flow of water over a dam). This should include the effect of the sedimentology described above as opposed to a simple heterogeneous debris mass. In this preliminary modelling, using both Geo-Slope 2003 [10] and its incorporated packages, SEEP/W and SLOPE/W, an idealised rock-avalanche dam based upon the 1999 failure into the Poerua River, Westland, New Zealand involving 10–15 Mm^3 of schistose bedrock and colluvium [11, 12] is used. The Poerua rock-avalanche dam overtopped within 48 h but remained intact with flow confined in a relatively stable spillway with no obvious signs of erosion [11, 12]. The dam did, however, breach with an associated flood 6 days after emplacement after heavy rainfall. Preliminary modelling focuses on the emplacement of a dam that is relatively stable under normal flow conditions when overtopped, such as described initially for Poerua [11, 12]. Under these conditions the sedimentology of the dam becomes even more critical as the impounded lake fills as will be illustrated below. The modelling uses a 2-D section of a rock-avalanche dam at right

angles to the inferred runout direction of a rock avalanche that has crossed a narrow valley and completely blocked it. The section is at the lowest point of the dam crest, approximately 120 m high, with the lake impounded filling within 48 h to the overtopping point and then remaining at that maximum level. The dam is founded on schist bedrock with a valley gradient of 6°; the dam face is 24° downstream and 12° upstream, as at Poerua [11, 12]. The material properties of the dam are based upon GSD sampling carried out at Poerua and results in values of hydraulic conductivity for the carapace facies of 1.24×10^{-1} and 3.69×10^{-4} m/s for the body facies both equal in the x and y cartesian directions. For the preliminary modelling a comparison between a dam made entirely of the body facies and one consisting of the observed, but simplified sedimentology of a carapace and body facies is presented. Further details on the modelling conditions such as fitting data to a conductivity curve, the node spacing, strength, friction angles, volumetric water content function, and iteration conditions are to be discussed further in work in preparation.

An obvious exclusion to the modelling presented here is that of a dam formed only by the carapace facies. Preliminary results indicate that such a sedimentology is not suitable for forming a dam that can fill to overtopping since flow is able to move through the mass rapidly. However, assumptions for this form of sedimentology are common based on the surficial material presented to first investigators, and the assumption is dangerous that a lake will not form [9].

6.3 Seepage Analyses

Seepage analysis has been carried out using Geo-Slope (2003) SEEP/W [10], a finite element product to model movement and pore-water distribution within porous materials such as soil and rock. SEEP/W is able to model both saturated and unsaturated flow, the inclusion of unsaturated flow in groundwater modelling is important for obtaining physically realistic analytical results. SEEP/W accounts for the drainage of water from soil pores, or water filling soil pores, and the changes in hydraulic conductivity function that occur in a transient flow system. The computed head distribution can then be used in SLOPE/W slope stability analysis, particularly powerful in the case of transient systems.

6.4 Slope-Stability Analyses

Slope-stability analyses have been carried out using Geo-Slope (2003) SLOPE/W [10], a limit equilibrium theory based programme that calculates the factor of safety (FoS) for earth and rock slopes. Using limit equilibrium, it has the ability to model heterogeneous soil types, complex stratigraphic and slip surface geometry, and variable pore-water pressure conditions using a large selection of soil models. Analyses can be performed using deterministic or probabilistic input parameters. Porewater pressure conditions can be specified in SLOPE/W in several ways, including finite

element computed porewater pressures. SLOPE/W has the ability to import porewater pressure data computed by SEEP/W, VADOSE/W or SIGMA/W, three of GEO-SLOPE's finite element programs. This capability is especially useful for performing slope stability analyses where the groundwater flow conditions are transient and/or significantly affected by the stress state within the soil. In this case the computed head distribution for each time increment in SEEP/W has been imported into SLOPE/W to determine the FoS as a function of time as the impounded lake fills to overtopping and beyond, for the two sedimentological models. The style of failure in use is interpreted to be of a form that would remove the dam crest allowing for a catastrophic breach. Larger failures that remove the entire dam in one failure are deemed an unlikely occurrence. A brief summary of conditions derived, and through approximation with known materials, yields cohesion of zero for both facies, a unit weight of 20 kN/m^2 and a friction angle close to the maximum angle of repose at the dam, 24° as the "worst credible" value.

More complex modelling has been carried using FLAC (produced by Itasca) in which the failure surface evolves naturally, and in all cases is curved but FoS values and the depths of failure approximate well to the GEO-SLOPE values for the simplified purposes of this paper and so these results are presented.

6.5 Modelling Results

6.5.1 Single Facies Model

Seepage analysis shows a typical progressive saturation front for a homogenous earth dam with a steadily filling impounded lake. Figure 19.10 shows the position of the phreatic surface at 6 h intervals from the commencement of lake filling until 12 h after the lake had reached crest level. Progression is initially rapid, due to the filling of the lake and associated rising head on the upstream face. As the lake level

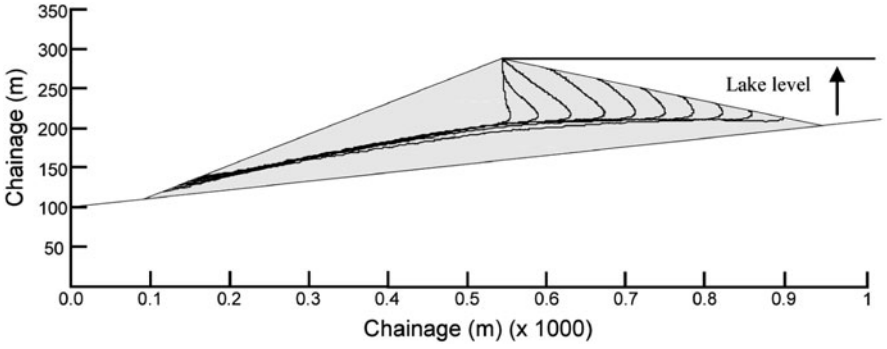

Fig. 19.10 Six hourly positions of the phreatic surface within a single facies dam from 0 to 60 h. Note the steady progression of the phreatic surface to overtopping and the presence of a low seepage point on the downstream dam face

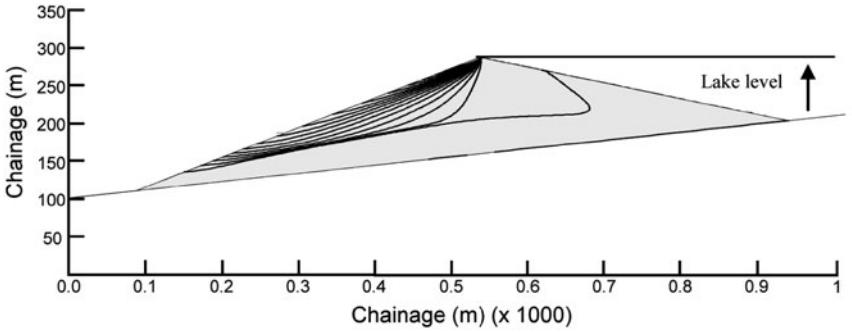

Fig. 19.11 Forty hourly positions of the phreatic surface within a single facies dam from 0 to 720 h. Note the steadily increasing position of the seepage point on the downstream dam face

reaches the dam crest, the rate of progression of the phreatic surface lowers as the driving head reduces within the embankment with distance from the downstream face to the phreatic surface. After 720 h, the seepage has not yet reached steady state, however the phreatic surface has progressed sufficiently to cause a reduction of the FoS to below unity. Figure 19.11 shows the progression of the saturation front at 40 h intervals to 720 h.

6.5.2 Simplified Observed Facies Model

In this case seepage analysis shows an identical progressive saturation front to 38 h. Figure 19.12 shows the positions of the phreatic surface at 2 h intervals from the commencement of lake filling until the lake has reached crest level. After 38 h, the lake level has reached the carapace facies. As the lake level rises above the carapace, the phreatic surface progresses more rapidly through the carapace than through the less permeable body facies. This results in a downstream "tonguing"

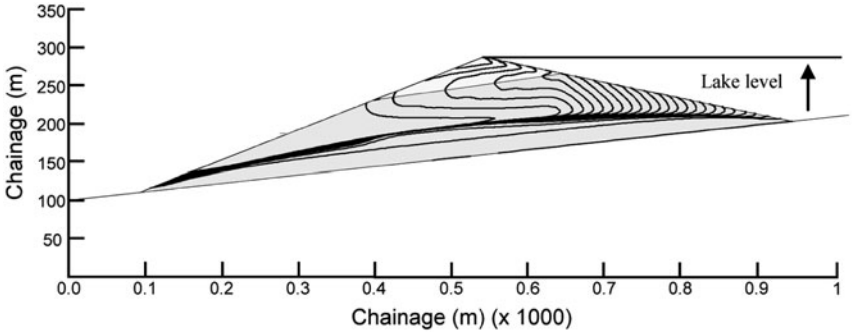

Fig. 19.12 Two hourly positions of the phreatic surface within a two facies dam from 0 to 48 h. Note the rapid advance of the surface once the lake level reaches the carapace facies and the high point on the downstream dam face that seepage occurs

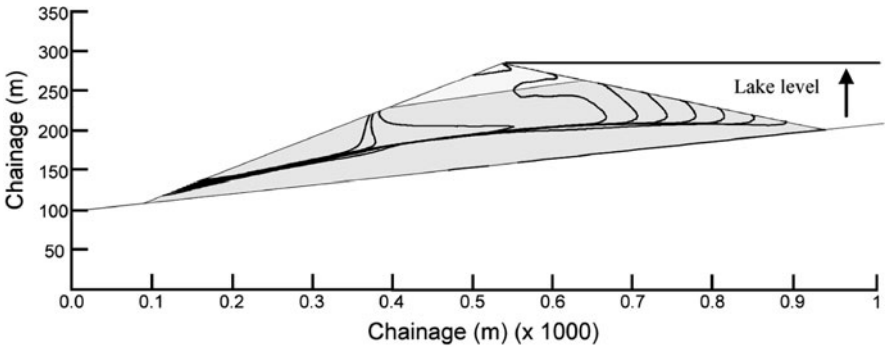

Fig. 19.13 Six hourly position of the phreatic surface within a two facies dam from 0 to 60 h. The carapace facies offers virtually no resistance to flow in comparison with the body facies and the phreatic surface reacts accordingly

projection of the phreatic surface along, above, and slightly below the boundary between the body facies and the carapace facies. As the lake level approaches the dam crest, the saturation front progresses almost entirely through the carapace, and partially through the body. Figure 19.13 shows the positions of the phreatic surface at 6 h intervals from the start of the impounded lake filling until 12 h after the lake had reached crest level. After 48 h have passed, the carapace becomes entirely saturated, taking just 2 h to do so, and the saturation front continues to progress through the body up to 60 h. After 60 h, the seepage has not yet reached steady state, however the phreatic surface had progressed sufficiently to cause a reduction of the FoS to well below unity.

6.5.3 Slope Stability

Computed head distribution for time increments in the SEEP/W analyses were used in SLOPE/W slope stability analyses to determine the Factor of Safety as a function of time and therefore lake level. The resulting FoS are presented in Figs. 19.14 and 19.15 for the single and dual facies model respectively. The FoS computed were for a translational failure surface using a Morgenstern-Price analyses. The same failure surface has been used in each analysis, and approximately corresponds to the carapace facies – body facies contact, a likely failure level based on observational evidence of lake filling and dam failure sequences [9]. For both the 1 and 2 facies systems the FoS remains as 3.03 from 0 to 38 h. This represents the initial filling of the impounded lake up to the level of the failure surface, the phreatic surface has not progressed above the defined failure surface and so has no effect on the computed FoS. From 39 h onwards, the FoS reduces for each system as the phreatic surface progresses through the dam and also above the specified failure surface. The FoS for the two facies system reduces at a higher rate than for the 1 facies system, falling below unity after 49 h, the one facies system falls below unity after approximately 450 h.

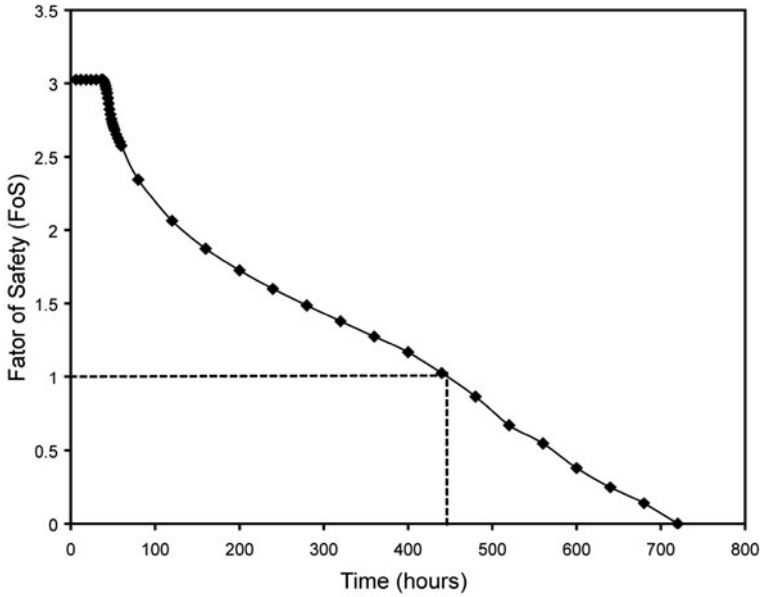

Fig. 19.14 Variation of the FoS of the rock-avalanche dam with time (lake level increase) using a specified block slide geometry and a Morgenstern-Price analysis method for a heterogeneous dam

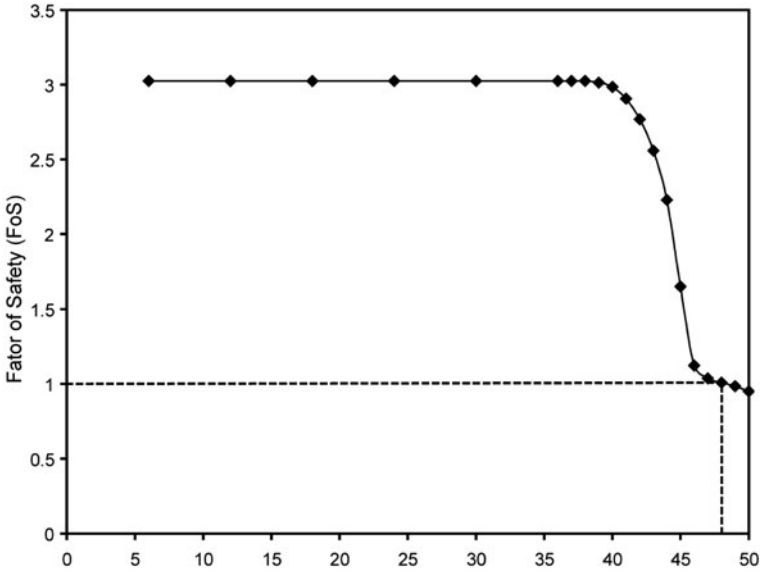

Fig. 19.15 Variation of the FoS of the rock-avalanche dam with time in hours (lake level increase) using a specified block slide geometry and a Morgenstern-Price analysis method for a dam showing a developed carapace and body facies

6.6 Discussion

Identical dam profiles and rates of external water level rise were used within the modelling of a simplified rock-avalanche dam. The same unit weight was specified for both the carapace facies and the body facies. Differences in the position of the saturation front, and therefore FoS between the 1 and 2 facies systems were controlled by the position of water within the embankment as controlled by the hydraulic conductivity and volumetric water content functions. The specification of a single facies dam results in failure after approximately 18.75 days. The introduction of a more permeable carapace facies in the upper third of the dam results in failure almost immediately after the lake reached the dam crest (48 h), due to the more rapid progression of the saturation front through the upper part of the dam. This is considerably quicker than the prototype; the Poerua dam maintained a "steady" overflow until heavy rainfall after a week allowed for failure, either through downstream face failure or head-cutting. The time to failure for the rock-avalanche dam modelled is directly related to the sedimentology specified. Using the observed sedimentology of the carapace and body faces instead of a homogenous mass results in a far more rapid failure of the upper third of the dam. This failure time is closely linked to the time of the impounded lake reaching the dam crest rather than just the body-carapace boundary. It is possible that this sort of failure mechanism is responsible for the observational evidence of rock-avalanche dams failing rapidly due to overtopping [3]. Future work will utilise more complex sedimentological models for modelling of dam response to lake filling and also more complex dam geometries. Of particular interest is the thickness and distribution of the carapace facies that appears to be key in the failure sequence. From a risk and hazard perspective, the location and development of downstream surface seeps is crucial. In a homogenous dam model the seep location gradually creeps up the downstream face; with a more realistic sedimentology the seep point is seen to rapidly rise up the dam face with increasing speed, and is an indicator of imminent risk of failure. Monitoring of such seepage points should form a basis of the hazard assessment of rock-avalanche dam failure.

7 Conclusions

This paper has outlined the sedimentology of rock-avalanche deposits, a common natural dam forming material. The results show a considerable advance on the current accepted knowledge of both the main fragmented interior of the deposit and the overall zonal structure; this includes evidence for the lack of crude inverse grading. This detailed sedimentology should form a vital part of any theory for the mechanism(s) of motion that allow(s) rock avalanches to travel for such excessive distances. As an example of the use of such sedimentological data, preliminary finite element and limit equilibrium modelling has been presented. Although simplified at present, the modelling shows the significant role that sedimentology can play in the

time of failure of a rock-avalanche dam. This variation in failure time has major consequences for hazard assessment and subsequent evacuation procedure. It has been shown that the monitoring of seepage fronts in terms of its progression up the downstream dam face could be a key indicator of internal sedimentology of the dam and lead to subsequent predictions of its stability. Numerous possibilities exist for future work related to this study. We must better constrain the variation in both rock-avalanche dam geometry and its effect, if any, on dam sedimentology. The pro-forma approach to sedimentology and stability using plots such as those presented in Figs. 19.8 and 19.9 can be developed to the point of lithological zonation reducing the need to sieve material and cut trenches.

In final summation, the sedimentology of rock-avalanche deposits should form a vital part of models for the processes during transport, and for the assessment of the post-emplacement behaviour of the resulting debris.

Acknowledgements This research and attendance of the NATO Advanced Research Workshop in 2004 from which this paper has developed was funded by the International Landslide Centre, University of Durham. The work was carried out in association with Dr. Tim Davies, Canterbury, New Zealand, and Dr. Mauri McSaveney, Geological and Nuclear Sciences, New Zealand, their help is much appreciated. The 2004 comments of the editorial committee when an earlier version of this paper was submitted are gratefully acknowledged.

References

1. Blott, S.J. and Pye, K. (2001) Gradistat: A grain size distribution and statistics package for the analysis of unconsolidated sediments, *Earth Surface Processes and Landforms* **26**, 1237–1248.
2. Casagli, N., Ermini, L. and Rosati, G. (2003) Determining grain size distribution of the material composing landslide dams in the Northern Apennines: Sampling and processing methods, *Engineering Geology* **69**, 83–97.
3. Costa, J.E. and Schuster, R.L. (1988) The formation and failure of natural dams, *Geological Society of America Bulletin* **100**, 1054–1068.
4. Crosta, G.B., Frattini, P. and Fusi, N. (2007) Fragmentation in the Val Pola rock avalanche, Italian Alps, *Journal of Geophysical Research – Earth Surface* **112**, F01006.
5. Cruden, D.M. and Hungr, O. (1986) The debris of the Frank Slide and theories of rockslide-avalanche mobility, *Canadian Journal of Earth Sciences* **23**, 425–432.
6. Davies, T.R., McSaveney, M.J. and Hodgson, K.A. (1999) A fragmentation-spreading model for longrunout rock avalanches, *Canadian Geotechnical Journal* **36**, 1096–1110.
7. Davies, T.R. and McSaveney, M.J. (2009) The role of rock fragmentation in the motion of large landslides, *Engineering Geology* **109**, 67–79.
8. Dunning, S.A., Mitchell, W.A., Rosser, N.J. and Petley, D.N. (2007) The Hattian Bala rock avalanche and associated landslides triggered by the Kashmir earthquake of 8 October 2005, *Engineering Geology* **93**, 130–144.
9. Dunning, S.A., Rosser, N.J., Petley, D.N. and Massey, C.I. (2006) Formation and failure of the Tsatichhu landslide dam, Bhutan, *Landslides* **3**, 107–113.
10. Geo-Slope (2003) Geo-Slope Office (SLOPE/W, SEEP/W, QUAKE/W). Geo-Slope International, Calgary, AB.
11. Hancox, G.T., McSaveney, M.J., Davies, T.R., Hodgson, K. and Daniel, R. (2000) The October 1999 landslide dam in Poerua River, Westland, New Zealand., New Zealand Society on Large Dams (NZSOLD) Symposium, November 2000.

12. Hancox, G.T., McSaveney, M.J., Manville, V.R. and Davies, T.R. (2005) The October 1999 Mt. Adams rock avalanche and subsequent landslide dam-break flood and effects in Poera River, Westland, New Zealand, *New Zealand Journal of Geology and Geophysics* **48**, 683–705.
13. Hewitt, K. (1998) Catastrophic landslides and their effects on the Upper Indus streams, Karakoram Himalaya, northern Pakistan, *Geomorphology* **26**, 47–80.
14. Hewitt, K., Clauge, J.J. and Orwin, J.F. (2008) Legacies of catastrophic rock slope failures in mountain landscapes, *Earth Science Reviews* **87**(1–2), 1–38.
15. Hooke, R.L. and Iverson, N.R. (1995) Grain-size distribution in deforming subglacial tills: Role of grain fracture, *Geology* **23**, 57–60.
16. Hungr, O. and Evans, S.G. (2004) Entrainment of debris in rock avalanches: An analysis of a long runout mechanism, *Geological Society of America Bulletin* **116**, 1240–1252.
17. Korup, O., Clague, J.J., Hermanns, R.L., Hewitt, K. and Strom, A.L. (2007) Giant landslides, topography, and erosion, *Earth and Planetary Science Letters* **261**(3–4), 578–589.
18. McSaveney, M.J. and Davies, T.R. (1999) The Falling Mountain rock avalanche of 1929, Arthur's Pass National Park, New Zealand, Institute of Geological and Nuclear Sciences Science Report, 15 pp.
19. Sammis, C.G., White, P., Osborne, R.H., Anderson, J.L. and Banerdt, M. (1986) Self-similar cataclasis in the formation of fault gouge, *Pure and Applied Geophysics* **124**, 53–78.
20. Schneider, J.-L., Wassmer, P. and Ledésert, B. (1999) The fabric of the sturzstrom of flims (Swiss Alps): Characteristics and implications on the transport mechanisms, *Earth and Planetary Sciences* **328**, 607–613.
21. Smith, G.M., Davies, T.R. and McSaveney, M.J. (2006) The Acheron rock avalanche, Canterbury, New Zealand – morphology and dynamics, *Landslides* **3**(1), 62–72.
22. Strom, A.L. and Pernick, L.M. (2004) Utilisation of the data on rockslide dams formation and structure for blast-fill dams design, in K. Abdrakhmatov, S.G. Evans, R. Hermanns, G. Scarascia Mugnozza, and A.L. Strom (eds.) Security of natural and artificial rockslide dams, extended abstracts, NATO Advanced Research Workshop, Bishkek, Kyrgyzstan, June 8–13, 2004, 177–182.
23. Weibull, W. (1951) A statistical distribution function of wide applicability, *Journal of Applied Mechanics* **18**, 837–843.
24. Wen, B., Aydin, A. and Duzgoren-Aydin, N.S. (2002) A comparative study of particle size analyses by sieve-hydrometer and laser diffraction methods, *Geotechnical Testing Journal* **25**, 1–9.
25. Wright, C.A. (1998) The AD 930 long-runout Round Top debris avalanche, Westland, New Zealand, *New Zealand Journal of Geology and Geophysics* **41**, 493–497.